Base Station Antenna Pattern Distortion in Practical Urban Deployment Scenarios

Rodriguez Larrad, Ignacio; Nguyen, Huan Cong; Sørensen, Troels Bundgaard; Franek, Ondrej

Published in:
Vehicular Technology Conference (VTC Fall), 2014 IEEE 80th

DOI (link to publication from Publisher):
10.1109/VTCFall.2014.6965887

Publication date:
2014

Document Version
Accepted author manuscript, peer reviewed version

Base Station Antenna Pattern Distortion in Practical Urban Deployment Scenarios

Ignacio Rodriguez[1], Huan C. Nguyen[1], Troels B. Sørensen[1], Ondrej Franek[2]

[1]Radio Access Technology Section (RATE)
[2]Antennas, Propagation and Radio Networking Section (APNET)
Department of Electronic Systems, Aalborg University, Denmark
{irl, hcn, tbs, of}@es.aau.dk

***Abstract*—In real urban deployments, base station antennas are typically not placed in free space conditions. Therefore, the radiation pattern can be affected by mounting structures and nearby obstacles located in the proximity of the antenna (near-field), which are often not taken into consideration. Also the intrinsic propagation mechanisms of the urban environment (far-field) can contribute to the distortion of the radiation pattern observed in a practical deployment scenario, especially when comparing it to the antenna pattern provided by the manufacturer and typically measured in free space. This paper presents a combination of near-field and far-field simulations aimed to provide an overview of the distortion experienced by the base station antenna pattern in two different urban deployment scenarios: rooftop and telecommunications tower. The study illustrates how, in comparison with the near-field effects, the urban propagation becomes the main contributor to the total distortion experienced. For the considered scenarios, the simulation results show a front-to-back-ratio reduction of approximately 10-15 dB in the effective antenna pattern compared to the free space reference. The near-field distortion has been evaluated by means of finite integration technique (FIT) simulations, while the far-field effects have been analyzed through intelligent ray tracing (IRT).**

I. Introduction

According to heterogeneous network (HetNet) deployment strategies, macro base station (BS) densification is the initial solution adopted by mobile network operators to cope with the growing traffic demand before beginning the deployment of small cells [1]. By increasing the number of BS, the inter-site distance is reduced. This causes an increase of the number of interfering BSs, and therefore, radio planning plays an important role in order to keep a good performance of the network. In general, radio planning tools consider a number of different BS parameters such as height, orientation, downtilt and antenna pattern. All these parameters are crucial for an accurate coverage prediction or determination of exclusion zones for human exposure [2]. Especially important is the antenna pattern, which is typically imported into the tools directly from the specifications of the manufacturer combined with a set of thresholds that prevent the presence of unrealistic nulls in the pattern by limiting the maximum dynamic range and thereby the front-to-back ratio (FBR). However, there are further aspects that, typically, are not considered as for example the distortion of the antenna pattern due to the metallic mounting structures and the different obstacles located in the vicinity of the antenna. This near-field (NF) distortion, together with the different far-field (FF) urban propagation mechanisms (e.g. diffraction and reflection), can cause the effective radiation pattern of the BS antenna to differ significantly from the antenna pattern measured in free space conditions. As a reference, the measurement studied in [3] reported an approximate reduction of 5-20 dB in FBR with respect to the specifications from the BS antenna manufacturer in a practical 3G urban deployment.

Little work has been reported in the literature about the distortion of BS antenna patterns. One of the first approaches [4] was a theoretical study of the edge diffraction suffered by the fields of an arbitrary aperture antenna in a finite ground plane. This work found insignificant variations in the azimuth plane and up to 4-5 dB ripples in the elevation back lobe. Other studies [5, 6] estimated the effect of different antenna masts, reflectors and mounting structures by applying array-theory and method-of-moments (MoM) techniques. The first study found a 1.5-3 dB variation in the antenna boresight direction due to presence of the masts. The second one, found a negligible distortion caused by mounting structures, a reduction in the side lobe of the vertical radiation pattern of an array antenna due to masts, an up to 10 dB distortion in the azimuth plane due to 5 cm thick masts and, up to 10 dB variations due to building roofs when the antenna was not correctly oriented. A more recent publication [7] presented the analysis of chimneypot-like radomes for 3G BS antennas by means of finite-difference time-domain (FDTD) simulations reporting a FBR reduction of 2-4 dB depending on the shape of the radome.

In order to complement the previous work, this paper presents a combination of advanced NF and FF simulations which allows to understand the contribution of each of the different sources, including propagation, to the total distortion in two simple but realistic urban deployments: rooftop and telecommunications tower. The proposed analysis method is closely related to the one presented in [8], where different spherical wave models, antenna models and ray-tracing were used. Differently in this case, in order to provide a complete and accurate approach, the distortion caused

Fig. 1. Typical urban BS deployments considered in the paper: a) rooftop, b) telecommunications tower.

by NF elements such as mounting structures and nearby obstacles is studied by means of finite integration technique (FIT) electromagnetic simulations; meanwhile the distortion caused by FF propagation mechanisms has been evaluated through intelligent ray tracing (IRT) simulations. An original contribution in this paper is to show the impact of the different sources on the average received power as function of angle.

The remaining of the paper is organized as follows: Section II presents an overview of different urban BS deployments and introduces the two scenarios considered in this paper. Section III gives an overview of the simulation environment and the different parameters used in the design of the scenarios. In Section IV, the results are presented and discussed, and finally, Section V provides a conclusion.

II. Practical Urban Base Station Deployments

In typical urban deployments, BSs are located in elevated positions to cover large areas. Ideally, the radio signal propagates above rooftops, gets diffracted at rooftop edges, and is guided by the street canyons (by multiple reflections on buildings and corner diffractions) until it reaches the user terminal. In general, the radio planning tools used by mobile operators are able to model the propagation to some extent. They typically model mainly the average field strength, but not the complex realistic propagation based on the 3D geometry of the scenario. Also, they do not consider the elements located in the vicinity of the BS antenna (e.g. mounting structures and nearby obstacles). Two practical urban BS deployments have been selected in this paper for studying and comparing the distortion suffered by the radiation pattern under different configurations: rooftop and telecommunications tower.

A. Rooftop Deployment

This is possibly the most relevant scenario for typical urban deployments. As it is illustrated in Fig. 1a, there can be several potential sources of NF distortion above rooftops: the other two antennas of the tri-sector, antenna mounting structures, camouflage radomes for low visual impact [9], the rooftop floor, and any other obstacle on the rooftop (e.g. chimneys).

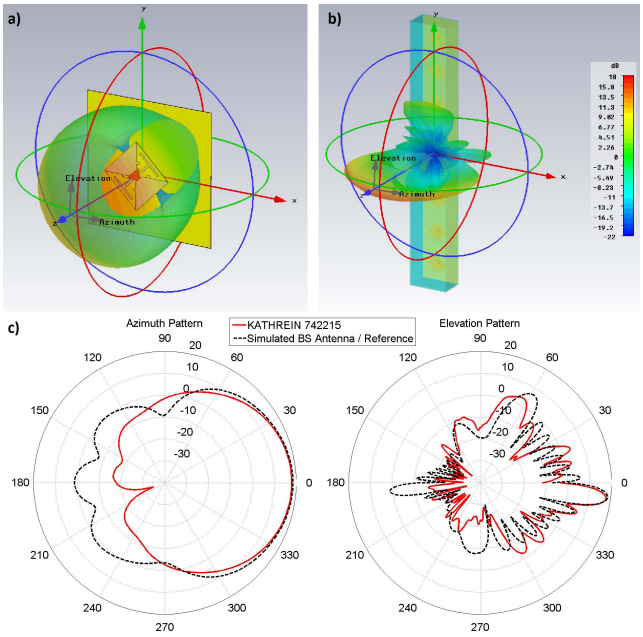

Fig. 2. Some details from the BS antenna design in CST: a) antenna element, b) designed BS and 3D radiation pattern, c) 2D radiation patterns of the designed BS compared to Kathrein 742215.

B. Telecommunications Tower Deployment

In the case of the telecommunications tower in Fig. 1b, due to its metallic character, the main contributor to the NF distortion is the tower itself, together with other antennas and mounting structures.

III. Numerical Simulations

All the NF simulations presented in the paper have been carried out with CST Microwave Studio [10], based on FIT computation techniques. On the other hand, WinProp, the radio propagation and network planning tool from AWE Communications [11] has been used for FF simulations.

A. Near-Field FIT Simulations

In order to recreate the BS antenna Kathrein 742215 [12] used in the deployments studied in [3], a simple 8-element array antenna was designed based on the dual polarized patch element reported in [13]. This was done since the actual element type and number of elements used in the Kathrein antenna were unknown. The designed antenna is an example of BS antenna with a similar but not identical radiating performance to the Kathrein. An illustration of the considered antenna element and the designed BS antenna together with its 3D radiation pattern can be seen in Fig. 2a and Fig. 2b, respectively. Fig. 2c shows the matching to the Kathrein antenna in terms of azimuth and elevation radiation patterns for the considered frequency of 2200 MHz.

Table I summarizes the main parameters of the Kathrein and the simulated BS antennas. As it can be seen, both antennas are similar in terms of horizontal (H) and vertical (V) half-power beamwidth (HPBW), gain (G), first side lobe level (FSLL) and angle of downtilt.

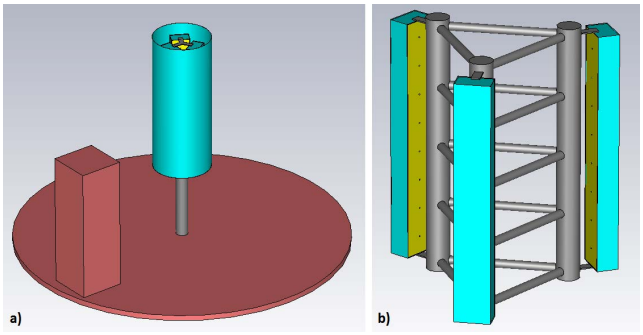

Fig. 3. Scenarios evaluated in CST: a) rooftop, b) telecommunications tower.

The different dimension (width) between both antennas is mainly due to the higher width of the antenna element used in the design of the simulated one. As it can be also noticed, the FBR of the simulated BS antenna does not meet the specification of the Kathrein antenna. Further refinements could have been done to the ground plane to improve this aspect during the BS antenna design stage, but since the main focus of the study is the analysis of the distortion, this is not considered as important issue, since the simulated BS antenna pattern is simply used as the reference for the different distortion calculations.

For the considered frequency, the wavelength (λ) is 0.1364 m and, consequently, the minimum FF distance (calculated as the Fraunhofer distance considering the largest dimension of the BS antenna) is approximately 6 m. As it can be seen in Fig. 1, there can be many elements surrounding the BS antenna inside the radiating NF zone. In order to analyze the distortion produced by some of these elements, the two scenarios considered were built in the simulation tool. The rooftop scenario has been modeled as a tri-sector inside a cylindrical radome mounted on a rooftop with a nearby chimney as it is shown in Fig. 3a. For this particular scenario, the different simulations allowed to quantify separately the distortion effects caused by each single element. For the telecommunications tower scenario, shown in Fig. 3b, a tri-sector mounted on a metallic tower has been modeled.

It is clear that different materials, sizes or distances between elements would impact the results. The main idea behind this study is to provide an indication of the contribution to the total distortion of different elements in practical deployments and, therefore, all the sizes, distances and materials of the different components are realistic and have been mainly selected based on the different mounting specifications detailed in [9] and [12].

TABLE I
COMPARISON OF BS ANTENNA PARAMETERS AT 2200 MHZ

PARAMETER	KATHREIN 742215	SIMULATED BS
H-HPBW	64°	65°
V-HPBW	6.4°	6.3°
FBR [180° ± 30°]	>30 dB	>20 dB
G	18 dBi	18.7 dBi
FSLL	-12 dB	-13 dB
Downtilt	7°	7°
Dimensions	1314 x 155 x 70 mm	1120 x 166 x 101 mm

TABLE II
FIT SIMULATION SETTINGS AND NF MODEL PARAMETERS

PARAMETER	VALUE
Solver	Time Domain
Grid Type	Hexaedral Mesh
Min. Resolution	$\lambda/10$
Radius tri-sector Rooftop	120 mm
Radius Cylindrical Radome	261 mm
Height Cylindrical Radome	1680 mm
Material Cylindrical Radome	Fiberglass 3 mm [14]
	$\epsilon_r = 4.4$, $tan\delta = 0.029$
Radius Pole Cylindrical Radome	55 mm
Height Pole Cylindrical Radome	750 mm
Material Pole Cylindrical Radome	Steel [10]
	$\mu_r = 1$, $\sigma = 6.993 \cdot 10^6$
Radius Rooftop Floor	1500 mm
Size of the Chimney	1200 x 400 x 400 mm
Position of the Chimney	15° Azimuth
Material Rooftop and Chimney	Concrete [10]
	$\epsilon_r = 4.5$, $tan\delta = 0.175$
Side Length Tower	543 mm
Radius Vertical Bars Tower	55 mm
Radius Horizontal Bars Tower	20 mm
Material Tower	Steel [10]
	$\mu_r = 1$, $\sigma = 6.993 \cdot 10^6$

Table II summarizes the main parameters used in the NF modeling and the FIT simulations. The outcome of all the different FIT simulations performed are the FF radiation patterns. By comparing them, the NF distortion caused by the different elements was computed in terms of azimuth and elevation pattern.

B. Far-Field IRT Simulations

In order to evaluate the contribution of urban propagation to the distortion, a IRT-based received power prediction [15, 16] was carried out in WinProp utilizing the different FF radiation patterns obtained from the simulations in CST as BS antenna patterns. The scenario considered is one of the locations investigated in [3]. At this location, the urban area is quite flat and regular with an average building height of 15-18 m (4-5 floors) and street width of approximately 20 m. The BS was placed on top of a building at 23 m height and its location and orientation are depicted in Fig. 4 by the black point and arrow. The black circle indicates the boundaries of the region over which the effective radiation pattern was computed.

One should understand the term effective pattern as the pattern observed under real deployment conditions. Ideally, it is the pattern that results from normalizing the (ensemble) average power received by a user circumscribing the base station at a fixed imaginary distance from the base station; the ensemble average is understood in respect to spatial averaging on the particular scenario under study, hence averaging both small-scale and local shadow fading effects. In practice, and especially in measurements, the spatial averaging is done over a small local area, sufficiently small so as not to introduce significant variations in received power due to change of angle or distance, and with proper compensation for large-scale distance effects to enable comparison of averages taken at different distances/angles. Typically, the distance range in which averages are taken is confined to the main beam direction in the elevation plane.

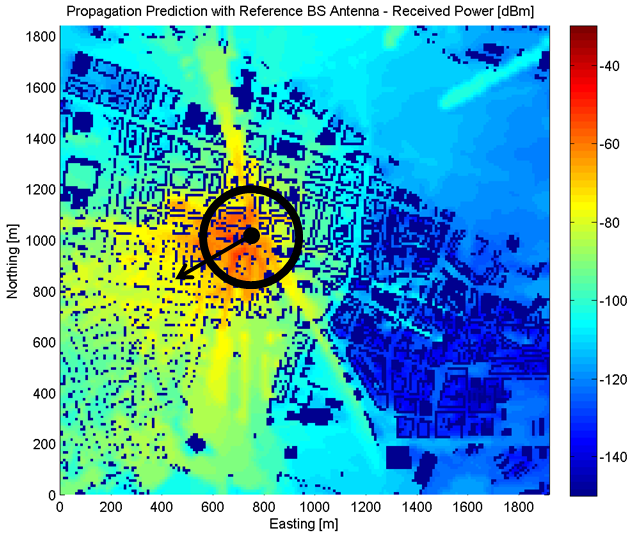

Fig. 4. Example of WinProp propagation prediction for the considered urban scenario. The black elements indicate BS location and orientation, and the distance range over which the effective pattern is computed.

In order to follow the previous indications, for this particular simulation analysis, the effective radiation pattern was computed at a reference distance of 175 m from the BS. This distance was calculated based on the geometry of the scenario considering the BS height (23 m), the height of the prediction (1.5 m) and the main beam elevation (7°).

With the aim of collecting enough representative samples to perform the aforementioned spatial averaging over small local areas, the data was collected in the range 175 ± 20 m. Inside this range the maximum large-scale variation of the samples is expected to be smaller than 4 dB, considering a non-line-of-sight (NLOS) path loss exponent of 4. For the estimation of the effective radiation pattern, the results are normalized to the average power value inside of a small $\pm 15°$ beamwidth in the boresight direction. The different parameters used in the IRT simulations are shown in Table III.

TABLE III
IRT SIMULATION SETTINGS

PARAMETER	VALUE
Resolution of 3D map	10 m
Transmit Power	33 dBm
Maximum Number of Rays	20
Reflection and Diffraction Losses	Empirical based on material
Maximum Number of Interactions	2 Reflections, 2 Diffractions, or 1 Reflection + 1 Diffraction
LOS Path Loss Exponent	2.9/4 before/after breakpoint
NLOS Path Loss Exponent	3.2/4 before/after breakpoint

IV. RESULTS AND DISCUSSION

A. Near-Field Distortion

Fig. 5 presents the azimuth and elevation radiation patterns obtained from the NF simulations performed. From the figure, it is possible to quantify the distortion introduced by the different elements considered in the two scenarios selected.

In the rooftop scenario, it can be seen how the cylindrical radome reinforces slightly the radiation in the back side (see increased gain compared to the reference in the regions around 150° and 210° in both azimuth and elevation). Despite typically these kind of low visual impact products are claimed to be RF-transparent, from the simulation an average back radiation increase of 1.27 dB in azimuth and 3.47 dB in elevation was found. This result is in line with the findings in [6] which predicted a FBR reduction of 2.43 dB for a circular radome of 650 mm of diameter.

Due to the geometry of the scenario, the rooftop itself distorts mainly to the elevation pattern, reducing the radiation in an average of 1.08 dB in the lower part (mainly the region between 210° and 330°). In the case a larger rooftop radius would have been considered in the simulation, the impact would have been extended towards elevation regions closer to the main lobe (centered at 353° due to the 7° of tilt). The impact of directing the main beam towards the rooftop was already studied in [5], and it is the equivalent of placing the BS antenna in a blind location in the middle of a rooftop without any simple radio planning consideration, so it can rarely occur.

Considering now a nearby obstacle, such as the chimney located in front of the active antenna of the tri-sector, it can be seen how, in azimuth, there is a reduction of approximately 3 dB in the radiation in the direction of the chimney (15°). A secondary effect, also in azimuth, of the nearby chimney is the reinforcement of the radiation in the back side due to the reflection of the signal on the chimney. This reinforcement in the back side is in average 2.37 dB.

In the telecommunications tower scenario, it can be seen how, according to the simulations, the most significant effect is the reduction in the back side of the azimuth pattern with an average decrement of 3.98 dB. Oppositely, in elevation, the back side radiation slightly reinforced in the regions around 150° and 210°. This distortion is dependent on the distance between the antenna and the mast of the tower and a higher distortion is expected for shorter distances as indicated in [5]. Table IV provides a detailed summary of the distortion caused by each of the different elements on the front and back radiation lobes.

TABLE IV
SUMMARY OF THE AZIMUTH AND ELEVATION DISTORTION CAUSED BY MOUNTING STRUCTURES AND NEARBY OBSTACLES

ELEMENT	AZIMUTH FRONT LOBE DISTORTION %-ile			AZIMUTH BACK LOBE DISTORTION %-ile		
	0%	50%	100%	0%	50%	100%
RADOME	-0.58 dB	-0.35 dB	-0.25 dB	-5.35 dB	0.73 dB	5.71 dB
ROOFTOP	-0.70 dB	-0.24 dB	0.54 dB	-2.04 dB	0.71 dB	3.73 dB
CHIMNEY	-3.08 dB	-1.79 dB	0.91 dB	-4.06 dB	0.51 dB	5.00 dB
TOWER	-0.38 dB	-0.07 dB	0.21 dB	-13.25 dB	-3.79 dB	2.83 dB

ELEMENT	ELEVATION FRONT LOBE DISTORTION %-ile			ELEVATION BACK LOBE DISTORTION %-ile		
	0%	50%	100%	0%	50%	100%
RADOME	-1.66 dB	-0.23 dB	2.62 dB	-6.19 dB	2.10 dB	14.81 dB
ROOFTOP	-1.12 dB	0.03 dB	2.92 dB	-17.43 dB	0.56 dB	9.78 dB
CHIMNEY	-5.54 dB	0.17 dB	11.78 dB	-10.86 dB	2.45 dB	12.33 dB
TOWER	-5.32 dB	-0.07 dB	1.66 dB	-11.12 dB	2.62 dB	21.36 dB

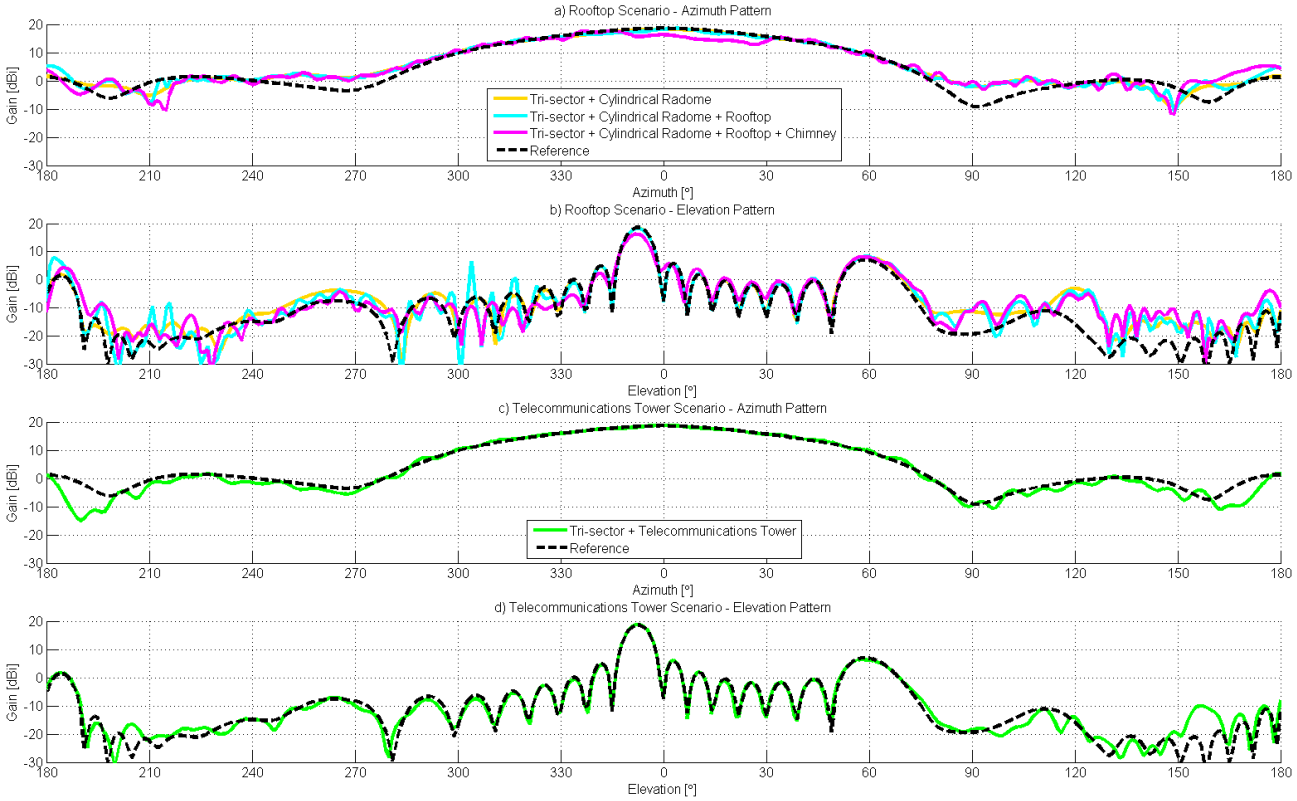

Fig. 5. Near-field distortion in azimuth and elevation for the different scenarios and elements considered.

These results combined with previous observations confirm that, in general, mounting structures and nearby obstacles have a small impact on the radiation pattern in agreement with [5], [6] and [7]. By considering the full rooftop scenario with radome plus rooftop and nearby chimney, the minimum azimuth FBR is reduced in 4.78 dB compared to the original reference of 20 dB. In the case of the telecommunications tower, the minimum azimuth FBR is minimally altered and remains close to the value of 20 dB.

B. Far-Field Propagation

Fig. 6 illustrates the effective radiation patterns estimated from the propagation predictions performed with the different BS antenna patterns. For simplicity, three cases are compared to the theoretical free space azimuth pattern. The first case (reference) corresponds to the propagation prediction done with the undistorted reference pattern. The second case considered is based on the full rooftop scenario distorted pattern which considers the influence of cylindrical radome plus rooftop plus nearby chimney. The last case considers the pattern distortion caused by the telecommunications tower.

As it can be seen, the effective patterns computed from the predictions with the distorted BS antenna patterns (rooftop and telecommunications tower scenarios) are very similar to the prediction with the original undistorted BS antenna pattern. This indicates, that despite of the different BS antenna patterns considered, the IRT simulations predict very similar ray propagation paths in the three cases.

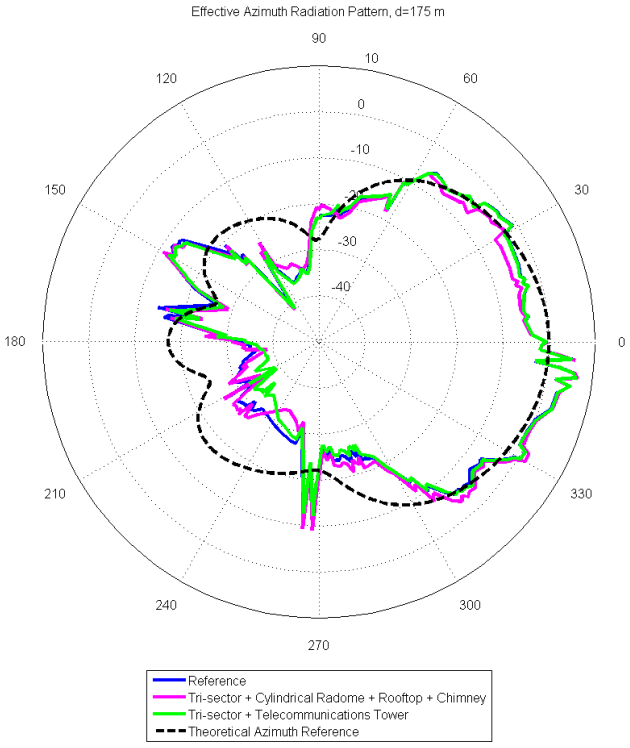

Fig. 6. Effective radiation pattern computed for the different scenarios.

The most remarkable difference between the three cases is the reduced/increased radiation of approximately 3 dB in the front/back side of the effective pattern computed in the rooftop case compared to the reference and the telecommunications tower cases. This is a consequence of the distortion caused by the chimney located in front of the BS antenna in the complete rooftop scenario previously analyzed.

In order to understand the magnitude of the distortion caused by the urban propagation effects, the effective patterns are also compared in Fig. 6 to the theoretical azimuth pattern previously presented in Section II. It can be seen how the front side of the effective patterns follow quite close the theoretical reference, while in the back side some increased radiation is observed (see region around 150°). From the urban geometry perspective, this effect can be explained as a strong contribution from the front lobe, reflected on a building and guided by the street canyons to the back side region. The minimum FBR for the different cases can be also deduced from the figure. In the case of the telecommunications tower and the reference cases, the minimum FBR is similar and approximately equal to 12.5 dB. In the case of the complete rooftop scenario, due to the previous observations, the minimum FBR is lower and equal to 11 dB. In both cases, this implies an approximate reduction of 10-15 dB from the original FBR, which confirms and explains the results from the measurement previously studied in [3].

Table V summarizes the distortion observed in the effective radiation patterns compared to the theoretical free space reference. Based on the magnitude of these FF distortion results compared to the NF distortion results presented in the previous subsection, it can be concluded that the urban propagation are the main contributors to the total antenna pattern distortion experienced in practical urban scenarios. This conclusion can be also reached by comparing the numbers given in Table VI, which gathers together all the different FBR results given along the section.

V. Conclusion

This paper presented a simulation-based analysis of the base station antenna pattern distortion experienced in two practical deployment scenarios: rooftop and telecommunications tower. The first part of the analysis, based on finite-integration-techniques, focused on the near-field distortion caused by mounting structures and nearby obstacles. The second part, based on intelligent ray-tracing, analyzed the distortion caused by the urban propagation mechanisms. The results show how, in general, the distortion produced by mounting structures and nearby obstacles is small compared to the contribution from the urban propagation. The biggest impact caused by elements inside the radiating NF zone was found for a rooftop chimney, which caused a front-to-back ratio reduction of approximately 4 dB. The combination of the different near-field distortion sources with the urban propagation effects leaded to a higher front-to-back ratio reduction of approximately 10-15 dB in the practical radiation pattern when comparing it to the free space reference pattern.

These results provide an explanation to previous studies from the literature and, as future work, a measurement campaign will be considered for a complete validation of the simulation results.

TABLE V
SUMMARY OF THE TOTAL DISTORTION OBSERVED FROM THE EFFECTIVE RADIATION PATTERN WITH RESPECT TO THE FREE SPACE REFERENCE

CASE	AZIMUTH FRONT LOBE DISTORTION %-ile			AZIMUTH BACK LOBE DISTORTION %-ile		
	0%	50%	100%	0%	50%	100%
REF	-4.77 dB	-0.60 dB	6.78 dB	-17.72 dB	-7.81 dB	7.73 dB
ROOFTOP	-5.19 dB	-1.63 dB	6.96 dB	-19.87 dB	-7.91 dB	8.68 dB
TOWER	-4.74 dB	-0.73 dB	6.69 dB	-19.25 dB	-12.39 dB	7.37 dB

TABLE VI
SUMMARY OF THE MINIMUM FBR CONSIDERING NF ELEMENTS AND PROPAGATION FOR THE DIFFERENT SCENARIOS.

SCENARIO	FBR,NF	FBR,FF
REF	>20 dB	>12.10 dB
ROOFTOP	>16.22 dB	>11.05 dB
TOWER	>20 dB	>12.37 dB

References

[1] Nokia Siemens Networks, "White Paper on Deployment Strategies for Heterogeneous Networks", May 2012.

[2] C. Oliveira, C.C. Fernandes and L.M. Correia, "Estimation of Exclusion Zones for Base Station Antennas in Wireless Communication Systems", *IEEE Vehicular Technology Conference*, Fall, 2007.

[3] S. Flores and M. Miñano, "Modelling of the Base Station Radiation Pattern in Practical Urban Deployment", Master Thesis, Aalborg University, June 2012.

[4] C.A. Balanis,"Pattern Distortion due to Edge Diffractions", *IEEE Transactions on Antennas and Propagation*, July 1970.

[5] A.F. Molisch, J. Fuhl and E. Bonek, "Pattern Distortion of Mobile Radio Base Station Antennas by Antenna Masts and Roofs", *European Microwave Conference*, 1995.

[6] A. Sarolic, B. Modlic and D. Poljak, "Analysis of a GSM Base Station Antenna near Conductive Object: Far Field Pattern Distortion", *International Conference on Applied Electromagnetics and Communications*, 2003.

[7] S. Finistauri, G. Marrocco, G. D'Orio, M. Motta, and S. De Polo, "Investigation on Pattern Distortion of Landsacape-Compliant 3G Base-Station Antennas", *IEEE Antennas and Propagation Society International Symposium*, 2004.

[8] M. Barbirolli, C. Carciofi, G. Falciasecca and M. Frullone, "Analysis of Field Strength Levels near Base Station Antennas"", *IEEE Vehicular Technology Conference*, Fall, 1999.

[9] Romkatel - ESB Systems, "Eco Site Low Visual Impact Antennas", http://www.romkatel.ro/cataloage/img/comob/esb_ecosite.pdf, Last Accessed: March 2014.

[10] CST - Computer Simulation Technology, "CST Studio Suite", http://www.cst.com/Products/CSTS2, Last Accessed: March 2014.

[11] AWE Communications, "Wave Propagation and Radio Network Planning", http://www.awe-communications.com/, Last Accessed: March 2014.

[12] Kathrein Inc. Scala Division, "742 215 X-Polarized 65^{o} Panel Antenna", http://www.kathrein-scala.com/catalog/742215.pdf, Last Accessed: March 2014.

[13] B. Li, Y.Z. Yin, W. Hu, Y. Ding and Y. Zhao, "Wideband Dual-Polarized Patch Antenna With Low Cross Polarization and High Isolation", *IEEE Antennas and Wireless Propagation Letters*, Vol. 11, 2012.

[14] K.L. Kaiser, "Electromagentic Compatibility Handbook", CRC Press, 2005.

[15] G. Wölfle , B.E. Gschwendtner and F.M. Landstorfer, "Intelligent Ray Tracing - A New Approach for Field Strength Prediction in Microcells", *IEEE Vehicular Technology Conference*, 1997.

[16] T. Rautiainen, G. Wölfle and R. Hoppe,"Verifying Path Loss and Delay Spread Predictions of a 3D Ray Tracing Propagation Model in Urban Environment", *IEEE Vehicular Technology Conference*, Fall 2002.